The Astrophysical Journal, 650:203–211, 2006 October 10

DIFFUSE, NONTHERMAL X-RAY EMISSION FROM THE GALACTIC STAR CLUSTER WESTERLUND 1

Michael P. Muno,[1,2] Casey Law,[3] J. Simon Clark,[4] Sean M. Dougherty,[5] Richard de Grijs,[6]
Simon Portegies Zwart,[7,8] and Farhad Yusef-Zadeh[3]
Received 2006 March 17; accepted 2006 June 19

ABSTRACT

We present the diffuse X-ray emission identified in *Chandra* observations of the young, massive Galactic star cluster Westerlund 1. After removing pointlike X-ray sources down to a completeness limit of $\approx 2 \times 10^{31}$ ergs s^{-1}, we identify $(3 \pm 1) \times 10^{34}$ ergs s^{-1} (2–8 keV) of diffuse emission. The spatial distribution of the emission can be described as a slightly elliptical Lorentzian core with a half-width at half-maximum along the major axis of $25'' \pm 1''$, similar to the distribution of point sources in the cluster, plus a $5'$ halo of extended emission. The spectrum of the diffuse emission is dominated by a hard continuum component that can be described as a $kT \gtrsim 3$ keV thermal plasma that has a low iron abundance ($\lesssim 0.3$ solar) or as nonthermal emission that could be stellar light that is inverse Compton scattered by MeV electrons. Only 5% of the flux is produced by a $kT \approx 0.7$ keV plasma. The low luminosity of the thermal emission and the lack of a 6.7 keV iron line suggest that $\lesssim$40,000 unresolved stars with masses between 0.3 and 2 $M_\odot$ are present in the cluster, fewer than previously estimated. Moreover, the flux in the diffuse emission is a factor of several lower than would be expected from a supersonically expanding cluster wind, and there is no evidence for thermal remnants produced by supernovae. Less than 10^{-5} of the mechanical luminosity of the cluster is dissipated as 2–8 keV X-rays, leaving a large amount of energy that either is radiated at other wavelengths, is dissipated beyond the bounds of our image, or escapes into the intergalactic medium.

Subject headings: stars: winds, outflows — supernova remnants — X-rays: ISM — X-rays: stars

1. INTRODUCTION

Sensitive X-ray observations are an increasingly important tool for studying young star clusters, particularly now that the *Chandra X-Ray Observatory* and the *XMM-Newton* X-ray Multi-Mirror Mission have made harder X-rays (2–10 keV) available for study. Young stars of all types are strong X-ray sources, with low-mass ($M < 3\ M_\odot$) pre–main-sequence stars producing X-rays in their active magnetic coronae (Preibisch & Feigelson 2005; Feigelson et al. 2005) and massive OB stars ($M \gtrsim 8\ M_\odot$) producing X-rays through shocks in their stellar winds (Chlebowski & Garmany 1991; Berghöfer et al. 1997; Skinner et al. 2002). Therefore, using observations of local star-forming regions (e.g., Orion) as templates, measurements of the integrated X-ray luminosities of more distant clusters can be used to constrain their total stellar population, including the numbers of young stars that may be unobservable in the optical and infrared because of extinction or source confusion (Feigelson et al. 2005; Nayakshin & Sunyaev 2005).

X-ray observations of clusters of massive stars also reveal diffuse X-ray emission that is produced as stellar winds encounter each other and the surrounding interstellar medium (ISM; e.g., Stevens & Hartwell 2003; Townsley et al. 2003, 2005[9], 2006; Law & Yusef-Zadeh 2004). Learning the fate of the energy carried by these winds, and eventually by supernovae, would provide insight into how galaxies evolve. If the energy is transferred to the ISM, it might at first trigger future generations of star formation, but a sufficiently large input of energy could clear away the ISM and halt star formation. Alternatively, if the energy escapes a galaxy, stellar winds and supernovae would enrich the intergalactic medium with metals. To determine the fate of that energy, it is necessary to obtain X-ray observations of clusters that have a range of ages and populations and that are surrounded by ISM with a variety of densities (e.g., Townsley et al. 2003, 2005).

In this paper we report on *Chandra* observations of the diffuse X-ray emission from the young Galactic star cluster Westerlund 1. The cluster contains 24 Wolf-Rayet (W-R) stars, more than 80 blue supergiants, at least 3 red supergiants, a luminous blue variable, and an amazing 6 yellow hypergiants, only 6 of which are known in the entire rest of the Galaxy (Westerlund 1987; Clark & Negueruela 2002, 2004; Negueruela & Clark 2005; Clark et al. 2005). Assuming a standard initial mass function (Kroupa 2002), Westerlund 1 could be as massive as $10^5\ M_\odot$, making it several times larger than the well-known, young Galactic clusters the Arches, Quintuplet, and NGC 3603. Westerlund 1 is also located only $\approx$5 kpc away (Clark & Negueruela 2002; Clark et al. 2005), so it is one of the closest young, dense star clusters. Therefore, Westerlund 1 is a crucial object for understanding the evolution of star clusters and their impact on the ISM of their host galaxies.

This is one of several papers describing the *Chandra* observations. In Muno et al. (2006), we reported the detection of a slow X-ray pulsar in Westerlund 1. Skinner et al. (2006) examined the X-ray emission from the W-R stars in the cluster, as well as a subset of the OB supergiants that are brightest in X-rays. In J. S. Clark et al. (2006, in preparation) we will report the spectroscopic identification of further optical counterparts to the X-ray

[1] Department of Physics and Astronomy, UCLA, Box 951547, Knudsen Hall, Los Angeles, CA 90095; mmuno@astro.ucla.edu.
[2] Hubble Fellow.
[3] Department of Physics and Astronomy, Northwestern University, 2131 Sheridan Road, Evanston, IL 60208.
[4] Department of Physics and Astronomy, Open University, Walton Hall, Milton Keynes MK7 6AA, UK.
[5] National Research Council, Herzberg Institute of Astrophysics, Dominion Radio Astrophysical Observatory, P.O. Box 248, Penticton, BC V2A 6K3, Canada.
[6] Department of Physics and Astronomy, University of Sheffield, Hicks Building, Hounsfield Road, Sheffield S3 7RH, UK.
[7] Astronomical Institute "Anton Pannekoek," Kruislaan 403, 1098 SJ Amsterdam, Netherlands.
[8] Section Computational Science, Kruislaan 403, 1098 SJ Amsterdam, Netherlands.

[9] Available at http://www.aoc.nrao.edu/events/xraydio.

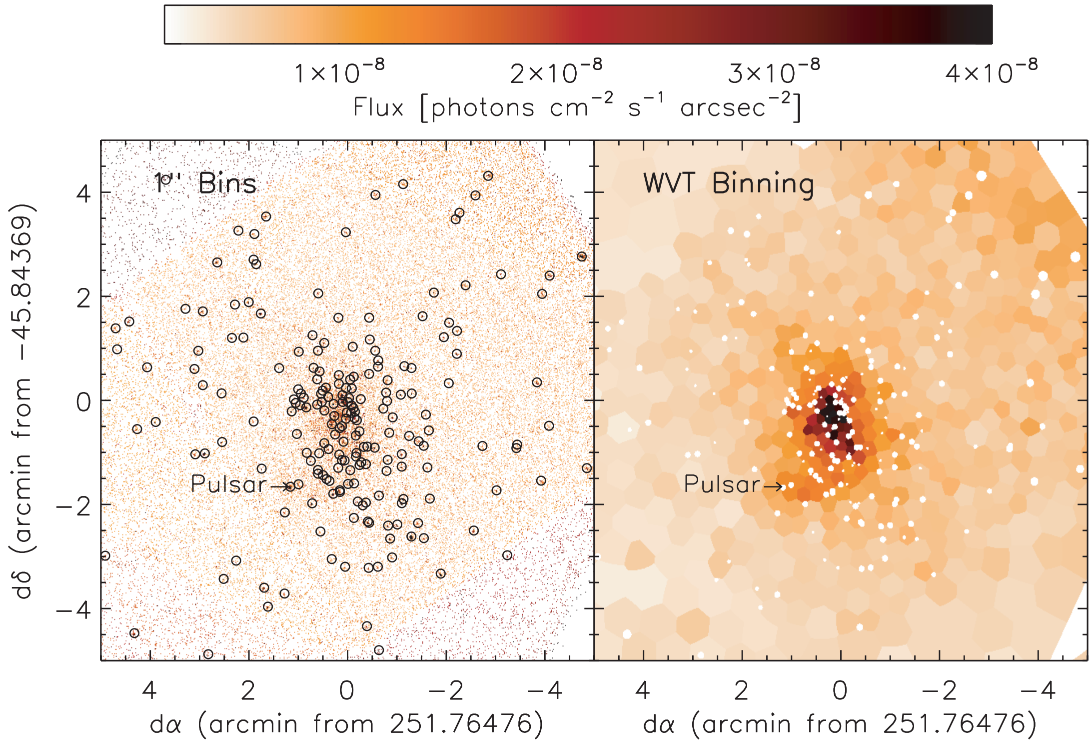

Fig. 1.—Images of the $10' \times 10'$ field around the center of Westerlund 1. *Left:* Unbinned image, with the pointlike X-ray sources described in J. S. Clark et al. (2006, in preparation) marked with circles. *Right:* Image of the diffuse X-ray emission in which the point sources have been excised and the image has been adaptively binned to a signal-to-noise ratio of 10 using the weighted Voronoi tessellation algorithm (Diehl & Statler 2006). The location of the 10.6 s X-ray pulsar (Muno et al. 2006) is also indicated.

sources and discuss the origin of the X-ray emission from these stars. In this paper we describe the spatial distribution (§ 2.1) and spectrum (§ 2.2) of the diffuse X-rays. We compare the emission seen from Westerlund 1 to that of other massive star clusters in the Local Group (§ 3). We suggest that Westerlund 1 is one of only a few star clusters to produce mostly nonthermal X-rays. We discuss the constraints that this places on the contributions of pre−main-sequence stars (§ 3.1), stellar winds (§ 3.2), and supernovae (§ 3.3) to the diffuse emission and examine what could be causing nonthermal emission (§ 3.4).

2. OBSERVATIONS AND DATA ANALYSIS

Westerlund 1 was observed with the *Chandra X-Ray Observatory* Advanced CCD Spectrometer Spectroscopic array (ACIS-S; Weisskopf et al. 2002) on two occasions: on 2005 May 22 for 18 ks (sequence 5411) and on 2005 June 20 for 42 ks (sequence 6283). We reduced the observation using standard tools that are part of CIAO version 3.3. We first created a composite event list for each observation. We corrected the pulse heights of the events to mitigate for the position-dependent charge transfer inefficiency using the standard CIAO process and excluded events that did not pass the standard *ASCA* grade filters and *Chandra* X-Ray Center (CXC) good-time filters. We searched for intervals during which the background rate flared to $\geq 3\ \sigma$ above the mean level and removed one such interval lasting 3.6 ks from sequence 5411. The composite image of the full field is displayed in J. S. Clark et al. (2006, in preparation); Figure 1 displays the inner $10'$ of the cluster at $1''$ resolution.

As described in J. S. Clark et al. (2006, in preparation), we identified pointlike X-ray sources in each observation using a wavelet-based algorithm, `wavdetect` (Freeman et al. 2002). In order to examine the diffuse X-ray emission, we then removed events that fell within circles circumscribing approximately 92% of the point-spread function (PSF) at the location of each point source and created an image using the remaining photons. Within $5'$ of the cluster core, 7386 counts were associated with known point sources, and 38,350 counts in diffuse emission, so photons from point sources in the wings of the PSF contribute only 0.5% to the diffuse flux.

2.1. *Spatial Distribution*

The signal-to-noise ratio in a $1''$ pixel was low, so we adaptively binned the image using the weighted Voronoi tessellation algorithm implemented by Diehl & Statler (2006), which is based on the algorithm of Cappellari & Copin (2003). The resulting image is displayed in the right panel of Figure 1.

In order to quantify the extent of the diffuse emission, we modeled its adaptively binned, two-dimensional spatial distribution (Fig. 1) as a Lorentzian function. Other functional forms used to model the light from star clusters also may be consistent with the data (e.g., Elson et al. 1987; Anders et al. 2006). However, there is little tradition in modeling the spatial distribution of diffuse X-rays from star clusters with analytic functions because that emission usually has a complex morphology (e.g., Townsley et al. 2003), so there is not an obvious choice for a functional form. We chose a Lorentzian function for its simplicity and because it is similar to the King models often used to quantify the distribution of optical light from star clusters (King 1962). The diffuse emission from Westerlund 1 is not circularly symmetric, so we allowed for an elliptical distribution defined as

$$f(x', y') = C + \frac{N}{1 + (x'^2 + \epsilon^2 y'^2)/r_0^2},$$
$$x' = (\alpha - \alpha_0)\cos\delta_0 \cos\theta + (\delta - \delta_0)\sin\theta,$$
$$y' = (\delta - \delta_0)\cos\theta - (\alpha - \alpha_0)\cos\delta_0 \sin\theta. \quad (1)$$

TABLE 1
Lorentzian Model of the Distribution of Diffuse X-Rays

Parameter	Value
C (10^{-8} photons cm^{-2} s^{-1})	0.53 ± 0.04
N (10^{-8} photons cm^{-2} s^{-1})	3.4 ± 0.2
α_0 (J2000.0)	16^h 47^m 4^s.3 ± 0^s.1
δ_0 (J2000.0)	−45° 50′ 59″ ± 1″
r_0 (arcsec)	25 ± 1
ϵ	0.75 ± 0.02
θ (deg)	13 ± 3
χ^2/ν	360/120

Note.—We define θ as positive for rotations east of north.

Here α_0 and δ_0 are the center of the distribution and x' and y' are the offset in arcseconds from the center, where the axes defining them have been rotated east of north by θ degrees. The remaining parameters are the background count rate C, the peak count rate N, the ellipticity of the distribution ϵ (a value of 1 implies a circle), and the characteristic radius of the distribution r_0. The final parameters and the goodness of fit χ^2/ν are listed in Table 1.

The fit is formally poor, with $\chi^2/\nu = 3$, because there are structures in the diffuse emission that cannot be described as part of an elliptical Lorentzian, including some bright knots of emission at the center of the cluster and a ridge of emission extending to the southeast toward the X-ray pulsar reported by Muno et al. (2006; it is also labeled in Fig. 1). However, the model does provide a useful means to quantify the azimuthally averaged distribution of the emission, as can be seen in the radial distribution, plotted in units of $r' = (x'^2 + \epsilon^2 y'^2)^{1/2}$, in Figure 2. The half-width at half-maximum of the distribution is 25″ ± 1″, which for a distance of 5 kpc corresponds to 0.5 pc. The widths of the distributions of both optical stars and pointlike X-ray sources are also ≈25″ (Clark et al. 2005; Muno et al. 2006). Moreover, the centroid of the diffuse emission lies within the 5″ uncertainty in the centroid of the point sources (Muno et al. 2006), although it is ≈20″ from the centroid of the optically detected stars (Piatti et al. 1998; Clark et al. 2005). The discrepancy could be caused either by differential extinction toward the cluster or by substructure in the cluster (J. S. Clark et al. 2006, in preparation).

In Figure 2 we have also indicated the amount of flux expected from the background of particles impacting the detector (1.5×10^{-9} photons cm^{-2} s^{-1}) and the mean flux taken from observations of the Galactic plane at $l = 28°$ and $b = 0.2°$ (2.2×10^{-9} photons cm^{-2} s^{-1}, of which half was particle background; see Ebisawa et al. 2005). Even 5′ from the cluster core, 60% of the flux was from Westerlund 1, so there is a broad halo of diffuse X-rays around the cluster. In contrast, although a few O stars that are cluster members are located beyond ~3′ from the cluster core (Clark et al. 2005), the surface density of X-ray point sources beyond 3′ is consistent with that of the Galactic disk (Muno et al. 2006), so there is no similar halo of pointlike X-ray sources.

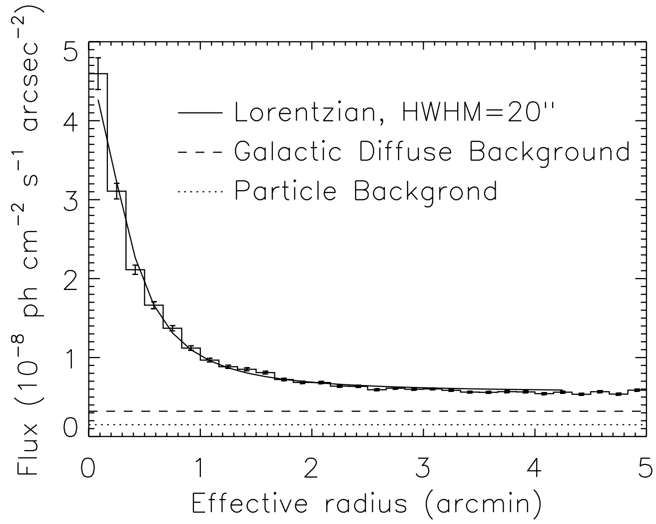

Fig. 2.—Radial profile of the diffuse X-ray emission (*histogram with errors*) along with the best-fit model described by eq. (1).

2.2. *Spectra*

Guided by Figure 2, we extracted spectra, response functions, and effective area curves for a circular 1′ region around the cluster center and annular regions 1′–2′, 2′–3′.5, and 3′.5–5′ from the cluster center. The background-subtracted spectra are displayed in Figure 3, in units of detector counts per square arcminute.

The spectra contained contributions from at least three sources of X-rays: plasma and unresolved stars in the cluster, diffuse emission from the Galactic plane, and events produced by particles incident on the detectors. The spectrum of the background from particles has been well characterized using observations in which the ACIS detectors were stowed out of the focal plane. Therefore, we subtracted the spectrum of the particle background from our source spectra. However, we were not able to make a local estimate of the Galactic emission because the cluster emission extended over the entire image. We have not attempted to subtract the Galactic plane emission from the spectra of the diffuse emission from Westerlund 1, but we have estimated the contribution of the Galactic emission by modeling a spectrum from observations of a field at $l = 28°$ and $b = 0.2°$ (Ebisawa et al. 2001, 2005).

We modeled the emission using version 12.2.0 of XSPEC (Arnaud 1996). We chose to model only the 1.5–8 keV energy range, for two reasons. First, the mean absorption column measured from the X-ray spectra of the point sources in Westerlund 1 is equivalent to 2×10^{22} cm^{-2} of hydrogen (J. S. Clark et al. 2006, in preparation). Therefore, most of the observed X-ray flux from the cluster should emerge at energies above ~2 keV, and the lower energy X-rays are probably from foreground emission. Second, given that the diffuse emission from Westerlund 1 is probably from several different sources, we do not have enough physical guidance to extrapolate our models below 2 keV. When we try to apply simple models, the inferred dereddened 0.5–2.0 keV flux can span an order of magnitude depending on the model assumptions. The lower bound was chosen to include the prominent line at 1.8 keV in the spectra from the inner 2′ of the cluster. For consistency with the other works quoted in § 3, we report the observed and dereddened 2–8 keV fluxes.

We first attempted to model the spectrum as a single-temperature thermal plasma, either in or out of collisional ionization equilibrium, absorbed by the ISM. We found that those simple models provided a poor description of the data from the inner 2′ of the cluster ($\chi^2/\nu \geq 1.5$).

Therefore, we modeled the spectra as an absorbed, two-temperature thermal plasma. Most of the 4–8 keV continuum flux could be modeled as a hot plasma with $kT_2 \gtrsim 3$ keV. In the inner 3′.5 of the cluster, the presence of emission lines near 1.8 keV from He-like Si and 2.3 keV from He-like S indicated that some of the flux is produced by a cool $kT_1 \lesssim 1$ keV plasma. The metal abundances in the cooler component were poorly

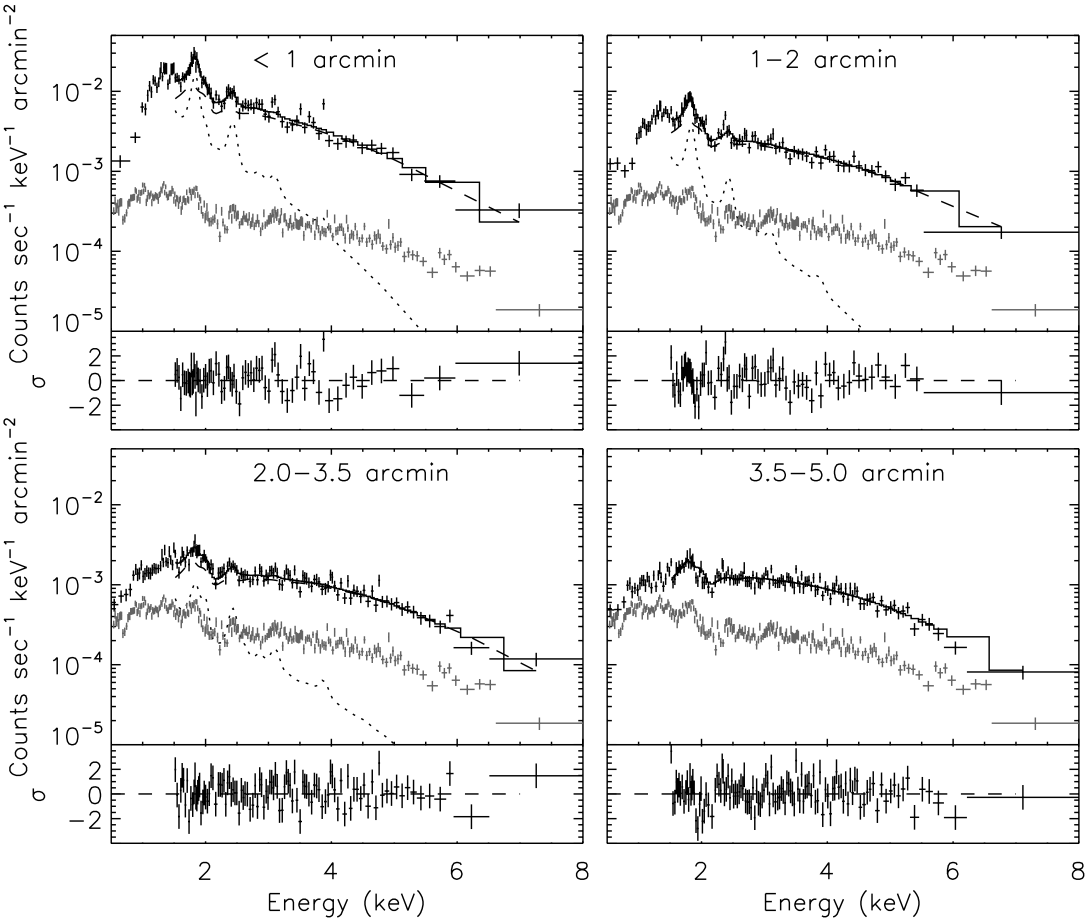

FIG. 3.—Background-subtracted spectra of the diffuse X-ray emission from Westerlund 1. In the top half of each panel, the spectra are plotted in detector units, so the intrinsic spectrum is still convolved with the response of the detector and telescope. The model spectrum is plotted with the solid histogram. The dotted line denotes the thermal component of the model, and the dashed line the nonthermal power-law component. The spectrum becomes noticeably harder farther from the cluster because the thermal component becomes weaker. The gray data points represent Galactic plane emission at $l = 28°$ and $b = 0.°2$, which contributes only 30% of the total flux toward Westerlund 1. In the bottom half of each panel, we plot the difference between the data and model normalized to the uncertainty (σ) in the data.

constrained because it contributes very little to the continuum emission, so we fixed the metal abundances to the mean best-fit value of $Z/Z_\odot = 2$. Moreover, the spectrum taken from the 3.′5–5.′0 annulus lacked obvious line emission, so the parameters of any cool plasma emission were unconstrained. Therefore, we omitted the cool component from the model of that spectrum. In Table 2 we list the parameters of the best-fit, two-temperature, collisional ionization equilibrium models; using nonequilibrium models yields similar results for the derived temperatures and abundances. Using these assumptions, the models were generally good descriptions of the data, with $\chi^2/\nu \approx 1$.

The most notable trend in the cool components is that their contributions to the spectra decline from 15% in the central 1′ to 7% between 1′ and 3.′5, finally becoming undetectable beyond 3.′5 from the cluster center. Otherwise, the inferred interstellar absorption remains roughly constant near 2.6×10^{22} cm^{-1}, and the temperature of the thermal component is constant near $kT \approx$ 0.7–1 keV. We find that the temperature of the hot plasma increases from $kT_2 = 3$ keV at the cluster center to a maximum of 11 keV in the 2.′0–3.′5 annulus and then decreases to 6 keV in the outer annulus. The relative lack of flux near the He-like Fe line at 6.7 keV in most of the spectra implies that the iron abundances are less than half of the solar values. Interestingly, similar subsolar iron abundances are inferred from the lack of 0.8–1.0 keV Fe L lines from several known Galactic W-R and O stars (e.g., Skinner et al. 2001, 2002, 2005; Schulz et al. 2003).

Alternatively, the lack of line emission near 6.7 keV could be explained if much of the continuum X-ray emission is nonthermal. Therefore, we have also modeled the emission as the sum of emission from a $kT \lesssim 1$ keV thermal plasma and a power law (Table 3). The metal abundances in the cooler component were once again fixed to $Z/Z_\odot = 2$, and we omitted the cool component from the model of the 3.′5–5′ annulus. This provides an equally good description of the data as the two-temperature plasma model, and the same trends are evident: the contribution of the cool component declines monotonically with offset from the cluster center, and the overall spectrum becomes harder.

The contributions of each model component under the second set of models are indicated in Figure 3, using dotted lines for the thermal plasma and dashed lines for the power-law component. We also display the spectrum of the Galactic ridge emission at $l = 28°$ and $b = 0.°2$ (*gray data points*). The line emission from the Galactic flux is a bit stronger than that from Westerlund 1, but otherwise the spectra are fairly similar. Therefore, we cannot completely rule out the hypothesis that the emission beyond $\approx 2'$ from the cluster core is Galactic. However, our assumption that the diffuse emission is from Westerlund 1 is conservative. As described in § 3, we find that the luminosity of diffuse X-rays from Westerlund 1 is much lower than expected, and assuming that the diffuse halo is Galactic would exacerbate the discrepancy.

The total, dereddened 2–8 keV flux from within 5′ of Westerlund 1 is 9.3×10^{-12} ergs cm^{-2} s^{-1}. By varying the

TABLE 2
Two-Temperature Plasma Model for the Diffuse X-Ray Emission

Parameter	<1′	1′–2′	2′.0–3′.5	3′.5–5′.0
Counts	4259	6679	12698	14714
Background	698	2244	5613	6636
Area (arcmin^2)	2.7	8.9	25.6	34.9
N_H (10^{22} cm^{-2})	$2.2^{+0.2}_{-0.2}$	$2.0^{+0.2}_{-0.2}$	$2.2^{+0.2}_{-0.2}$	$2.4^{+0.1}_{-0.1}$
kT_1 (keV)	$0.71^{+0.08}_{-0.12}$	$0.7^{+0.1}_{-0.1}$	$1.0^{+0.2}_{-0.2}$	...
$Z_1/Z_\odot$	2.0	2.0	2.0	...
$\int n_{e,1} n_{H,1}\, dV$ (cm^{-6} pc^3)	9^{+5}_{-2}	6^{+2}_{-1}	6^{+2}_{-2}	$^{+}_{-}$
kT_2 (keV)	$3.2^{+0.5}_{-0.4}$	$5.7^{+1.2}_{-0.8}$	11^{+4}_{-2}	$6.3^{+0.9}_{-0.8}$
$Z_2/Z_\odot$	<0.4	<0.3	$0.6^{+0.5}_{-0.4}$	<0.2
$\int n_{e,2} n_{H,2}\, dV$ (cm^{-6} pc^3)	16^{+3}_{-2}	17^{+1}_{-2}	24^{+2}_{-2}	43^{+1}_{-3}
χ^2/ν	73.4/65	80.4/72	104.9/101	129.1/116
F_X (10^{-13} ergs cm^{-2} s^{-1})	7.1 ± 0.9	11.3 ± 1.0	23.8 ± 2.0	27.0 ± 2.0
$uF_{X,1}$ (10^{-13} ergs cm^{-2} s^{-1})	1.5	0.9	2.0	...
$uF_{X,2}$ (10^{-13} ergs cm^{-2} s^{-1})	8.3	13.4	27.7	34.9

Notes.—Uncertainties are 1 σ, found by varying each parameter until $\Delta\chi^2 = 1.0$. Parameters $uF_{X,1}$ and $uF_{X,2}$ are the deabsorbed 2–8 keV flux from the thermal and nonthermal components of the spectral model, respectively. If we extrapolate our models to the 0.5–2.0 keV band, the rapidly increasing contribution from the $kT = 0.7$ keV thermal plasma causes the inferred X-ray luminosity to be a factor of 2–3 larger. Note also that at 5 kpc, $1' = 1.45$ pc.

assumptions in our model, we find that the systematic uncertainty in the 2–8 keV flux is ≈20%. Based on the *Chandra* observations taken at $l = 28°$ and $b = 0°.2$ (see also Ebisawa et al. 2005), we expect the Galactic emission to be 3×10^{-14} ergs cm^{-2} s^{-1} arcmin^{-2} (2–8 keV; see also Hands et al. 2004). Therefore, within 5′ of the core of Westerlund 1 the Galactic plane contributes ≈20% to the inferred flux. Subtracting this foreground and background emission and using a distance to Westerlund 1 of 5 kpc (Clark et al. 2005), we find that the luminosity of the diffuse X-ray emission from the cluster is $(3 \pm 1) \times 10^{34}$ ergs s^{-1} (2–8 keV). Only ≈5% of this luminosity is from the ≲1 keV thermal component.

3. DISCUSSION

The origin of the diffuse X-ray emission from clusters of massive young stars is currently under debate. Several authors (e.g., Cantó et al. 2000; Stevens & Hartwell 2003) have modeled the diffuse X-rays from the most massive clusters in the Local Group as a cluster wind. Under this model, the winds of individual stars collide, thermalize, and form a pressure-driven bulk flow that expands supersonically into the ISM (Chevalier & Clegg 1985). Stevens & Hartwell (2003) tabulated results from studies of R136, NGC 3603 (Moffat et al. 2002), NGC 346 (Nazé et al. 2002), the Rosette (Townsley et al. 2003), and the Arches (Yusef-Zadeh et al. 2002) and showed that the luminosities of their diffuse X-ray emission [$(1–6) \times 10^{34}$ ergs s^{-1}] were considerably larger than would be expected from the standard cluster wind model. The large X-ray luminosities can be explained several ways: the densities of the cluster winds could be higher than expected because the stellar winds entrained cooler material or because radiative losses decreased the temperature of the shocked plasma (Stevens & Hartwell 2003); the wind energy could be dissipated through heat conduction where it encounters nearby molecular clouds (Dorland & Montmerle 1987); or the winds could be confined by the surrounding ISM (Chu et al. 1995). Alternatively, the large X-ray luminosities might partly result from the fact that unresolved pre–main-sequence stars should contribute significantly to the luminosity of the (apparently) diffuse emission, especially for more distant clusters (e.g., Townsley et al. 2006).

Westerlund 1 is at least as massive as NGC 3603, R136, and the Arches (Clark et al. 2005), so from an observational standpoint the luminosity of its diffuse X-rays [$(3 \pm 1) \times 10^{34}$ ergs s^{-1}; 2–8 keV] is understandable. However, the spectrum and spatial distribution of the diffuse X-ray emission from Westerlund 1 present more of a puzzle. First, the spectrum lacks the line emission from He-like Fe that would be expected from a thermal plasma given the hard continuum flux. In contrast, the spectra of pre–main-sequence stars exhibit prominent lines from He-like and

TABLE 3
Thermal plus Nonthermal Model for the Diffuse X-Ray Emission

Parameter	<1′	1′–2′	2′.0–3′.5	3′.5–5′.0
N_H (10^{22} cm^{-2})	$2.7^{+0.3}_{-0.2}$	$2.3^{+0.3}_{-0.2}$	$2.4^{+0.2}_{-0.2}$	$2.8^{+0.3}_{-0.2}$
kT_1 (keV)	$0.68^{+0.10}_{-0.08}$	$0.68^{+0.09}_{-0.13}$	$1.1^{+0.2}_{-0.1}$	...
$Z_1/Z_\odot$	2.0	2.0	2.0	...
$\int n_e n_H\, dV$ (cm^{-6} pc^3)	11^{+4}_{-3}	$7.1^{+0.8}_{-1.8}$	6^{+2}_{-2}	...
Γ	$2.7^{+0.2}_{-0.2}$	$2.1^{+0.1}_{-0.2}$	$1.7^{+0.1}_{-0.1}$	$2.0^{+0.2}_{-0.1}$
N_Γ (10^{-3} photons cm^{-2} s^{-1} keV^{-1})	$1.0^{+0.3}_{-0.3}$	$0.7^{+0.2}_{-0.1}$	$0.8^{+0.1}_{-0.1}$	$1.7^{+0.4}_{-0.2}$
χ^2/ν	70.4/66	80.4/73	107.2/102	132.2/116
F_X (10^{-13} ergs cm^{-2} s^{-1})	7.2 ± 0.7	11.7 ± 1.0	23.1 ± 2.0	28.0 ± 2.0
$uF_{X,1}$ (10^{-13} ergs cm^{-2} s^{-1})	1.6	1.0	2.2	...
$uF_{X,2}$ (10^{-13} ergs cm^{-2} s^{-1})	9.0	14.2	27.2	37.3

Note.—See Table 2.

H-like Si, S, Ar, and Fe that imply metal abundances up to 10 times the solar value (e.g., Feigelson et al. 2005). However, X-ray spectra of O and W-R stars often exhibit weak Fe emission that implies abundances $\lesssim 0.3$ solar (e.g., Skinner et al. 2001, 2002, 2005; Schulz et al. 2003), so it is possible that the diffuse flux is dominated by plasma from the O and W-R star winds, with little contribution from pre–main-sequence stars. It is also possible that the diffuse emission is nonthermal, by analogy with similar interpretations for the hard flux from a handful of young stellar associations, including RCW 38 (Wolk et al. 2002), DEM L192 (N51D; Cooper et al. 2004), 30 Dor C (Bamba et al. 2004), and possibly the Arches cluster (Law & Yusef-Zadeh 2004). In most of the above cases, the nonthermal emission has been interpreted as synchrotron emission from supernova remnants. We examine this hypothesis for Westerlund 1 in § 3.4.

The second surprise is that the diffuse X-ray emission from Westerlund 1 seems to extend far beyond the core of the cluster. Within the inner $2'$, the surface brightness of the diffuse emission falls off with a half-width at half-maximum of 0.5 pc (Figs. 1 and 2), which is identical to the distribution of pointlike X-ray sources (J. S. Clark et al. 2006, in preparation). This core of diffuse emission could be produced either from the cluster wind, which radiates X-rays mostly in the region where the colliding winds are thermalized (Stevens & Hartwell 2003), or from an unresolved population of pre–main-sequence stars. However, between $2'$ and $5'$ (3–7 pc) from the cluster core the diffuse X-ray flux attains a constant level $\approx 7 \times 10^{-14}$ ergs cm^{-2} s^{-1} arcmin^{-2} (Table 2; Fig. 1), which is 2–3 times larger than is expected from the Galactic plane (e.g., Hands et al. 2004; Ebisawa et al. 2005). An expanding thermal plasma would exhibit a rapidly declining temperature profile, yet the spectrum of this halo of diffuse emission is quite hard and lacks the line emission expected from a cooling plasma. This makes it tempting to interpret the diffuse halo as nonthermal particles that are accelerated in a large-scale outflow.

Therefore, although the luminosity of the diffuse X-ray emission from Westerlund 1 is not surprising, the lack of line emission in the spectrum and broad spatial distribution of the diffuse X-rays is. To address this, in the following sections we quantify the probable contributions of pre–main-sequence stars, stellar winds, and supernovae to the X-ray emission from Westerlund 1.

3.1. *Unresolved Low-Mass Stars*

The nonthermal spectrum of the diffuse X-ray emission from Westerlund 1 puts interesting constraints on the population of low-mass stars in the cluster. The average spectrum of the lightly absorbed pre–main-sequence stars in Orion can be qualitatively described as a two-temperature plasma with $kT_1 = 0.5$ keV and $kT_2 = 3.3$ keV and with metal abundances of up to 10 times solar for S, Ar, Ca, and Fe (Feigelson et al. 2005). In contrast, in our models for the diffuse emission from Westerlund 1, a $kT \lesssim 1$ keV plasma contributes only 5% of the 2–8 keV diffuse X-ray flux, and the remaining hard flux does not exhibit the expected He-like Fe line at 6.7 keV, placing an upper limit on the Fe abundance of $\lesssim 0.3$ solar (Table 2). To obtain a conservative estimate of the number of low-mass stars in the cluster, we assume that they have solar Fe abundances (i.e., much lower abundances than the stars in Orion). We find that this implies that they produce $\lesssim 30\%$ of the diffuse flux from Westerlund 1, or $\approx 9 \times 10^{33}$ ergs s^{-1} (2–8 keV).

We use the results of the *Chandra* Orion Ultradeep Project (COUP) to convert this luminosity into a number of low-mass stars, taking into account the difference in ages between the two clusters. For Orion, the 1398 stars later than B4 in the COUP observations have an integrated, deabsorbed 2–8 keV luminosity of 1.2×10^{33} ergs s^{-1} (Feigelson et al. 2005). Most of this emission is produced by stars with $0.3\ M_\odot < M < 3\ M_\odot$.[10] However, the stars in Westerlund 1, with ages of ≈ 4 Myr (Clark et al. 2005), are significantly older than the 1 Myr old population in Orion. To take this into account, we first note that when 2–3 $M_\odot$ stars reach an age of ≈ 4 Myr, they become fully radiative and their X-ray luminosities drop by an order of magnitude (Flaccomio et al. 2003). Even though they are only 5% of low-mass stars by number, in Orion these 2–3 $M_\odot$ stars produce $\approx 30\%$ of the flux from $0.3\ M_\odot < M < 3\ M_\odot$ stars (see Fig. 4. of Feigelson et al. 2005), or $\approx 4 \times 10^{32}$ ergs s^{-1}. Second, Preibisch & Feigelson (2005) find that the X-ray luminosities of young stars with $0.5\ M_\odot < M < 2\ M_\odot$ fall off with time τ as $L_X \propto \tau^{-0.75}$, so at 4 Myr the stars in Orion should be ≈ 3 times fainter. Therefore, if Orion were 4 Myr old, we would expect its ≈ 1400 stars with $0.3\ M_\odot < M < 2\ M_\odot$ to have a luminosity of 3×10^{32} ergs s^{-1} (2–8 keV). Our upper limit to the integrated X-ray luminosity of low-mass stars in Westerlund 1 is $\lesssim 9 \times 10^{33}$ ergs s^{-1}, so we infer that Westerlund 1 contains $\lesssim 40{,}000$ stars with masses between $0.3\ M_\odot < M < 2\ M_\odot$.

This number of low-mass stars is smaller than one would expect if one were to extrapolate from the number of massive, post–main-sequence stars in the cluster using a standard initial mass function (Kroupa 2002). There are ≈ 150 stars brighter than $V = 21$ within $5'$ of the center of Westerlund 1, the faintest of which have recently been identified as O7 main-sequence stars that would have initial masses $\gtrsim 30\ M_\odot$ (J. S. Clark et al. 2006, in preparation). The maximum initial mass of the stars remaining in the cluster is uncertain because there is no precise means to determine the initial masses of the supergiants and W-R stars, but Clark et al. (2005) argue that it is probably in the range of 40–50 $M_\odot$. If we assume that the initial mass function can be described as a broken power law of the form $dN \propto M_i^{-\alpha}\, dM_i$, where $\alpha = 2.3$ for $M_i > 0.5\ M_\odot$ and $\alpha = 1.4$ for $0.3\ M_\odot < M_i < 0.5\ M_\odot$ (Kroupa 2002), then if there are 150 stars with $30\ M_\odot < M_i < 50\ M_\odot$, we would expect 100,000 stars with $0.3\ M_\odot < M < 2\ M_\odot$. This inferred lack of low-mass stars can be explained several ways. The slope of the initial mass function could be flat ($\alpha \lesssim 2.1$), as has been inferred for NGC 3603 and the Arches cluster based on infrared star counts (e.g., Eisenhauer et al. 1998; Stolte et al. 2005). The mass function could be truncated at low masses ($M < 0.6\ M_\odot$), by analogy with the fact that $M < 7\ M_\odot$ stars appear to be depleted in the Arches cluster (Stolte et al. 2005). Finally, the initial masses of the post–main-sequence stars in Westerlund 1 could span a much wider range of masses (20–60 $M_\odot$) than assumed in Clark et al. (2005).

If we assume that the mass function is truncated at low masses, the total mass of the cluster would not differ significantly from the estimate of $10^5\ M_\odot$ in Clark et al. (2005) based on the unmodified Kroupa form. However, if the mass function is flat, or the optically detected stars had a wider range of initial masses, the total mass of the cluster would be only 40,000–70,000 $M_\odot$. Obviously, an accurate measurement of the mass function, and consequently the total mass, requires direct infrared observations of the low-mass stars in Westerlund 1. However, these X-ray observations provide a useful starting point.

3.2. *Stellar Winds*

It is not clear whether stellar winds or supernovae are the dominant source of the diffuse X-ray emission from Westerlund 1

[10] The COUP sample of X-ray sources is complete to $\approx 0.2\ M_\odot$, and excluding the singularly bright O6 star θ^1 Ori C (with a luminosity of 3×10^{32} ergs s^{-1} [2–8 keV], it could be detected as a point source in our observations of Westerlund 1), the $>3\ M_\odot$ stars in Orion produce only $\approx 6\%$ of the integrated X-ray luminosity.

because it is at an age when both should contribute equally to its mechanical output (e.g., Leitherer et al. 1992). Individual stellar winds carry a power of

$$L_w = 3 \times 10^{35} \left(\frac{\dot{M}}{10^{-6}\ M_\odot\ \mathrm{yr}^{-1}} \right) \left(\frac{v_w}{10^3\ \mathrm{km\ s}^{-1}} \right)^2 \mathrm{ergs\ s}^{-1}, \quad (2)$$

where $\dot{M}$ is the mass-loss rate and v_w is the wind velocity. The W-R stars dominate the mechanical output from stellar winds, with typical $\dot{M} \approx 6 \times 10^{-5}\ M_\odot\ \mathrm{yr}^{-1}$ and $v_w \approx 1700\ \mathrm{km\ s}^{-1}$, so that $L_w \approx 5 \times 10^{37}\ \mathrm{ergs\ s}^{-1}$ (Leitherer et al. 1992). With 24 W-R stars in the cluster, the total mechanical energy output from winds is $>1 \times 10^{39}\ \mathrm{ergs\ s}^{-1}$.

We can estimate the X-ray luminosity of the resulting cluster wind using the analytic solutions to the density and temperature that Cantó et al. (2000; see also Stevens & Hartwell 2003) derived for a wind expanding supersonically into the ISM (Chevalier & Clegg 1985). Within the radius of the cluster where the stars input their energy, the density is given by

$$n_0 = 0.1N \left(\frac{\dot{M}_w}{10^{-5}\ M_\odot\ \mathrm{yr}^{-1}} \right) \left(\frac{v_w}{10^3\ \mathrm{km\ s}^{-1}} \right)^{-1} \left(\frac{R_c}{\mathrm{pc}} \right)^{-2} \mathrm{cm}^{-3} \quad (3)$$

(note that we used the supersonic solution with an adiabatic index $\gamma = 5/3$ for the original equation) and the temperature by

$$kT_0 = 1.3 \left(\frac{v_w}{1000\ \mathrm{km\ s}^{-1}} \right)^2 \mathrm{keV}, \quad (4)$$

where N is the number of stars, $\dot{M}_w$ is the average mass-loss rate of the stars, and R_c is the radius within which the stars are contained and the winds are thermalized. If we use the values above for W-R stars, assume $N = 24$, and take the radius of the cluster to be $R_c = 4$ pc ($\approx 3'$ at 5 kpc), then we find $n_0 = 0.6\ \mathrm{cm}^{-3}$ and $kT_0 = 4$ keV. Using any of the standard plasma models in XSPEC (e.g., Mewe et al. 1986; Liedahl et al. 1995), and converting n_0 and R_c to an emission measure [i.e., $K_{\mathrm{EM}} = (4/3)\pi R_c^3 n_0^2$], we find a predicted $L_X = 3 \times 10^{34}\ \mathrm{ergs\ s}^{-1}$ (2–8 keV). Therefore, a cluster wind could in principle account for all of the diffuse X-rays from Westerlund 1.

However, the cluster wind model is not able to account for the spatial distribution of the diffuse X-rays from Westerlund 1. A cluster wind would produce almost all of the diffuse X-ray emission within the core radius R_c (Stevens & Hartwell 2003), whereas 70% of the diffuse emission from Westerlund 1 is part of a halo that extends out to at least $5'$ (Fig. 2). If we consider only the core of the diffuse emission as originating from stellar winds, then the cluster is underluminous by a factor of 2.

This result is particularly surprising given that the standard cluster wind model applied by Stevens & Hartwell (2003) to NGC 3603, R136, and NGC 346 predicted significantly *less* flux than is observed. In those cases, Stevens & Hartwell (2003) favored the hypothesis that cold material was being entrained in the wind. To reconcile our results for Westerlund 1 to the cluster wind model, we would have to assume that enough cold material is entrained that the cluster wind no longer emits in the 2–8 keV bandpass. This requires that the plasma be cooled by a factor of ≈ 10, to $\lesssim 0.4$ keV. Based on Figure 1 of Stevens & Hartwell (2003), we estimate that this would require that the mass of cold material input into the wind is twice that of the hot material, or roughly $3 \times 10^{-3}\ M_\odot\ \mathrm{yr}^{-1}$. The mass-loss rates from the ≈ 10 luminous blue variables, red supergiants, and yellow hypergiants, which should be $<10^{-4}\ M_\odot\ \mathrm{yr}^{-1}$ each (e.g., Jura & Kleinmann 1990; Leitherer et al. 1992; Smith et al. 2004), probably could not account for this large amount of cool mass. Therefore, either there is a currently unseen source of mass in Westerlund 1, or the stellar winds are not thermalized within the cluster and escape without radiating much.

3.3. *Supernovae*

The presence of an isolated X-ray pulsar in Westerlund 1 (Muno et al. 2006) confirms that supernovae have occurred there. If we extrapolate an initial mass function with slope $\alpha = 1.8$–2.7 for $M > 30\ M_\odot$ to higher masses, we expect that the cluster originally contained ≈ 80–150 stars with initial masses $>50\ M_\odot$ that have already undergone supernovae. For the most massive stars, this would have started when the cluster was about 3 Myr old, so the average supernova rate over the last 1 Myr should be on order one every 7000–13,000 yr. If each supernova had a kinetic energy of 10^{51} ergs, then the average power released by supernovae is $\sim(2$–$5) \times 10^{39}\ \mathrm{ergs\ s}^{-1}$.

No obvious supernova remnant is present in our *Chandra* image of Westerlund 1, but this is not surprising. We have examined images from the *Spitzer* GLIMPSE program (R. Indebetouw 2006, private communication), and there is no evidence that dense gas or dust still surrounds Westerlund 1. Therefore, Westerlund 1 appears to have cleared away the ISM for parsecs around. When a supernova occurs in such an evacuated cavity, a typical radio and X-ray remnant is not expected until the remnant encounters the boundaries of the bubble blown by the cluster (e.g., Ciotti & D'Ercole 1989).

Whether the hard, possibly nonthermal emission from Westerlund 1 is produced by supernovae is unclear. Most supernova remnants produce thermal X-ray emission with strong lines, but a few are also nonthermal X-ray sources. For example, RCW 86 and SN 1006 exhibit nonthermal filaments near the outer boundary of the shock and thermal emission in the interior (e.g., Dyer et al. 2004; Rho et al. 2002). AX J1843.8−0352 and G346.3−0.5 exhibit nonthermal emission almost exclusively throughout the remnant (e.g., Ueno et al. 2003; Lazendic et al. 2005; Hiraga et al. 2005). Unfortunately, there is not a satisfactory explanation as to why a small fraction of supernova remnants produce nonthermal emission, so the issue remains unresolved for Westerlund 1.

3.4. *Nonthermal Particles*

In principle, nonthermal particles can be produced either in supernova remnants (e.g., Lyutikov & Pohl 2004) or in colliding stellar winds (e.g., Eichler & Usov 1993). Once they are produced, inverse Compton scattering should dominate synchrotron losses by a large factor in Westerlund 1 (see, e.g., Rybicki & Lightman 1979). The ratio of the energy-loss rates is given by the ratio of the background radiation to the magnetic energy density. The energy density of the stellar light from the OB and W-R stars in Westerlund 1 is approximately

$$\begin{aligned} U_{\mathrm{phot}} &= \frac{L_{\mathrm{stars}}}{4\pi c D^2} \\ &= 5.5 \times 10^{-9} \left(\frac{L_{\mathrm{stars}}}{10^7\ L_\odot} \right) \left(\frac{d}{1\ \mathrm{pc}} \right)^{-2} \mathrm{ergs\ cm}^{-3}, \quad (5) \end{aligned}$$

where $L_{\mathrm{stars}} \sim 10^7\ L_\odot$ is the luminosity of the cluster. For synchrotron losses to be important, magnetic fields would have to have an energy of $B^2/8\pi \gtrsim U_{\mathrm{phot}}$, which corresponds to $B \gtrsim 0.4$ mG. This is much stronger than the microgauss fields generally assumed for the ISM (e.g., Beck 2001), so inverse Compton scattering is probably the dominant loss mechanism for nonthermal particles.

If the nonthermal X-ray emission is produced by inverse Compton scattering, the energy requirements are modest. Nonthermal particles would only need to be replenished at a rate sufficient to balance the X-ray luminosity, 3×10^{34} ergs s^{-1}. Furthermore, inverse Compton scattering photons from optical and UV energies ($E_{\rm in}$ = 2–20 eV) into the X-ray band ($E_{\rm out} \approx$ 3 keV) only requires electrons with $\gamma^2 \sim E_{\rm out}/E_{\rm in}$, or energies of 6–20 MeV. These particle energies are rather small. For comparison, if the magnetic field in Westerlund 1 has a strength of only 10 μG, producing nonthermal synchrotron radio emission like that seen from 30 Dor C (Bamba et al. 2004) requires electrons with energies of a few GeV. Therefore, detecting diffuse, nonthermal radio emission from a star cluster like Westerlund 1 (e.g., Yusef-Zadeh et al. 2003) would provide a much more interesting constraint on the maximum energies of particles than detecting nonthermal X-rays. The interferometric radio observations in the literature (Clark et al. 1998) would have resolved out arcminute-scale diffuse radio emission, so single-dish observations are necessary to determine whether higher energy particles are also produced by the cluster.

4. SUMMARY

We have identified diffuse X-ray emission within 5′ of the core of Westerlund 1 with a modest luminosity of $(3 \pm 1) \times 10^{34}$ ergs s^{-1} (2–8 keV). This low luminosity is puzzling because unresolved pre–main-sequence stars, a thermalized cluster wind, or a series of supernova remnants would each be expected to produce at least this much X-ray emission. Therefore, one or all of these mechanisms are not producing nearly as much X-ray flux as would be expected based on comparison with other star clusters and with theoretical calculations.

The lack of a 6.7 keV He-like Fe line accompanying the hard 4–8 keV continuum implies that no more than 30% of the diffuse emission is produced by young stellar objects. Therefore, we infer that there are $\lesssim$40,000 stars with masses between 0.3 and 2 $M_{\odot}$, which is significantly fewer than the 10^5 stars one would expect from extrapolating the number of massive, optically identified stars to lower masses using a standard initial mass function (Clark et al. 2005). Moreover, this limit is conservative because in computing it we have assumed that the line emission from the low-mass stars would be produced by a solar abundance of iron. If we had assumed that iron had an abundance several times the solar value, as it does in the spectra of stars in Orion (Feigelson et al. 2005), then only a few percent of the diffuse 2–8 keV flux could be produced by pre–main-sequence stars.

In contrast, the lack of iron emission in the spectrum is consistent with a similar underabundance of iron that is observed in X-ray spectra of individual O and W-R stars (e.g., Skinner et al. 2001, 2002, 2005; Schulz et al. 2003). However, if the O and W-R star winds collide and thermalize as expected, they would form a pressure-driven cluster wind that would expand and cool rapidly (Cantó et al. 2000; Stevens & Hartwell 2003). Such a wind would not radiate in the X-ray band outside of the cluster core and therefore cannot explain the broad halo of emission between ≈3′ and 5′.

Instead, the halo of X-rays may represent nonthermal particles accelerated by the colliding stellar winds or by supernova remnants. However, the energy lost in X-rays represents less than 10^{-5} of the kinetic energy released by stellar winds and supernova remnants. The rest of the energy either (1) emerges below 2 keV where our observations are insensitive, (2) dissipates beyond the bounds of our image (≈7 from the cluster core) when the cluster wind or supernova remnants impact the ISM, or (3) escapes the Galactic plane, enriching the intergalactic medium with metals. We plan to address the second option in the next year, by observing a larger area around the cluster (≈15′) with *XMM-Newton*.

Support for this work was provided by the National Aeronautics and Space Administration through Chandra Award 06400311 issued by the *Chandra* X-Ray Center, which is operated by the Smithsonian Astrophysical Observatory for and on behalf of the National Aeronautics Space Administration under contract NAS8-03060. Support for M. P. M. was provided by NASA through Hubble Fellowship grant HST-HF-01164.01-A awarded by the Space Telescope Science Institute, which is operated by the Association of Universities for Research in Astronomy, Inc., for NASA, under contract NAS 5-26555.

REFERENCES

Anders, P., Gieles, M., & de Grijs, R. 2006, A&A, 451, 375
Arnaud, K. A. 1996, in ASP Conf. Ser. 101, Astronomical Data Analysis Software and Systems V, ed. G. Jacoby & J. Barnes (San Francisco: ASP), 17
Bamba, A., Ueno, M., Nakajima, H., & Katsuji, K. 2004, ApJ, 602, 257
Beck, R. 2001, Space Sci. Rev., 99, 243
Berghöfer, T. W., Schmitt, J. H. M. M., Danner, R., & Cassinelli, J. P. 1997, A&A, 322, 167
Cantó, J., Raga, A. C., & Rodríguez, L. F. 2000, ApJ, 536, 896
Cappellari, M., & Copin, Y. 2003, MNRAS, 342, 345
Chevalier, R. A., & Clegg, A. W. 1985, Nature, 317, 44
Chlebowski, T., & Garmany, C. D. 1991, ApJ, 368, 241
Chu, Y.-H., Chang, H.-W., Su, Y.-L., & Mac Low, M.-M. 1995, ApJ, 450, 157
Ciotti, L., & D'Ercole, A. 1989, A&A, 215, 347
Clark, J. S., Fender, R. P., Waters, L. B. F. M., Dougherty, S. M., Koornneef, J., Steele, I. A., & van Blokland, A. 1998, MNRAS, 299, L43
Clark, J. S., & Negueruela, I. 2002, A&A, 396, L25
———. 2004, A&A, 413, L15
Clark, J. S., Negueruela, I., Crowther, P. A., & Goodwin, S. P. 2005, A&A, 434, 949
Cooper, R. L., Guerrero, M. A., Chu, Y.-H., Chen, C.-H. R., & Dunne, B. C. 2004, ApJ, 605, 751
Diehl, S., & Statler, T. S. 2006, MNRAS, 368, 497
Dorland, H., & Montmerle, T. 1987, A&A, 177, 243
Dyer, K. K., Reynolds, S. P., & Borkowski, K. J. 2004, ApJ, 600, 752
Ebisawa, K., Maeda, Y., Kaneda, H., & Yamauchi, S. 2001, Science, 293, 1633
Ebisawa, K., et al. 2005, ApJ, 635, 214
Eichler, D., & Usov, V. 1993, ApJ, 402, 271
Eisenhauer, F., Quirrenbach, A., Zinnecker, H., & Genzel, R. 1998, ApJ, 498, 278
Elson, R. A. W., Fall, S. M., & Freeman, K. C. 1987, ApJ, 323, 54
Feigelson, E. D., et al. 2005, ApJS, 160, 379
Flaccomio, E., Damiani, F., Micela, G., Sciortino, S., Harnden, F. R., Murray, S. S., & Wold, S. J. 2003, ApJ, 582, 398
Freeman, P. E., Kashyap, V., Rosner, R., & Lamb, D. Q. 2002, ApJS, 138, 185
Hands, A. D. P., Warwick, R. S., Watson, M. G., & Helfand, D. J. 2004, MNRAS, 351, 31
Hiraga, J. S., Uchiyama, Y., Takahashi, T., & Aharonian, F. A. 2005, A&A, 431, 953
Jura, M., & Kleinmann, S. G. 1990, ApJS, 73, 769
King, I. 1962, AJ, 67, 471
Kroupa, P. 2002, Science, 295, 82
Law, C., & Yusef-Zadeh, F. 2004, ApJ, 611, 858
Lazendic, J. S., Slane, P. O., Gaensler, B. M., Reynolds, S. P., Plucisnky, P. P., & Hughes, J. P. 2005, ApJ, 618, 733
Leitherer, C., Robert, C., & Drissen, L. 1992, ApJ, 401, 596
Liedahl, D. A., Osterheld, A. L., & Goldstein, W. H. 1995, ApJ, 438, L115
Lyutikov, M., & Pohl, M. 2004, ApJ, 609, 785
Mewe, R., Lemen, J. R., & van den Oord, G. H. J. 1986, A&AS, 65, 511
Moffat, A. F. J., et al. 2002, ApJ, 573, 191
Muno, M. P., et al. 2006, ApJ, 636, L41

Nayakshin, S., & Sunyaev, R. 2005, MNRAS, 364, L23
Nazé, Y., Hartwell, J. M., Stevens, I. R., Corcoran, M. F., Chu, Y.-H., Koenigsberger, G., Moffat, A. F. J., & Niemela, V. S. 2002, ApJ, 580, 225
Negueruela, I., & Clark, J. S. 2005, A&A, 436, 541
Piatti, A. E., Bica, E., & Clariá, J. J. 1998, A&AS, 127, 423
Preibisch, T., & Feigelson, E. D. 2005, ApJS, 160, 390
Rho, J., Dyer, K., Borkowski, K. J., & Reynolds, S. P. 2002, ApJ, 581, 1116
Rybicki, G., & Lightman, A. 1979, Radiative Processes in Astrophysics (New York: Wiley)
Schulz, N., Canizares, C., Huenemoerder, D., & Tibbits, K. 2003, ApJ, 595, 365
Skinner, S. L., Güdel, M., Schmutx, W., & Stevens, I. R. 2001, ApJ, 558, L113
Skinner, S. L., Simmons, A. E., Zhekov, S. A., Teodoro, M., Damineli, A., & Palla, F. 2006, ApJ, 639, L35
Skinner, S. L., Zhekov, S. A., Güdel, M., & Schmutz, W. 2002, ApJ, 572, 477
Skinner, S. L., Zhekov, S. A., Palla, F., & Barbosa, C. L. D. R. 2005, MNRAS, 361, 191
Smith, N., Vink, J. S., & de Koter, A. 2004, ApJ, 615, 475
Stevens, I. R., & Hartwell, J. M. 2003, MNRAS, 339, 280
Stolte, A., Brandner, W., Grebel, E. K., Lenzen, R., & Lagrange, A.-M. 2005, ApJ, 628, L113
Townsley, L. K., Broos, P. S., Feigelson, E. D., Brandl, B. R., Chu, Y.-H., Garmire, G. P., & Pavlov, G. G. 2006, AJ, 131, 2140
Townsley, L. K., Feigelson, E. D., Montmerle, T., Broos, P. S., Chu, Y.-H., & Garmire, G. P. 2003, ApJ, 593, 874
Townsley, L. K., Feigelson, E. D., Montmerle, T., Broos, P. S., Chu, Y.-H., Garmire, G., & Getman, K. 2005, in X-Ray and Radio Connections, ed. L. O. Sjouwerman & K. K. Dyer
Ueno, M., Bamba, A., Koyama, K., & Ebisawa, K. 2003, ApJ, 588, 338
Weisskopf, M. C., Brinkman, B., Canizares, C., Garmire, G., Murray, S., & van Speybroeck, L. P. 2002, PASP, 114, 1
Westerlund, B. E. 1987, A&AS, 70, 311
Wolk, S. J., Bourke, T. L., Smith, R. K., Spitzbart, B., & Alves, J. 2002, ApJ, 580, L161
Yusef-Zadeh, F., Law, C., Wardle, M., Wang, Q. D., Fruscione, A., Lang, C. C., & Cotera, A. 2002, ApJ, 570, 665
Yusef-Zadeh, F., Nord, M., Wardle, M., Law, C., Lang, C., & Lazio, T. J. W. 2003, ApJ, 590, L103